MINERALOGICAL ANALYSIS OF CALCIUM-ALUMINUM-RICH INCLUSIONS PROVIDES INSIGHT INTO POST-FORMATION PROCESSES. V.E. Burnette[1,2], P. Mane[1], and T. Erickson[3] [1]Lunar and Planetary Institute (USRA), Houston, TX 77085, [2]The University of Texas at Austin, Austin, TX 78705, [3]Jacobs-JTS, NASA Johnson Space Center, Houston, TX 77085.

Introduction: Calcium-aluminum inclusions (CAIs) are cm- to mm-sized intergrowths of refractory phases found in chondritic meteorites [1]. Their mineral compositions closely match the compositions of the solids thought to condense from an extremely hot (>1500K) gas with a bulk solar composition [2-4], suggesting that CAIs were the earliest solids within the Solar System [2-4]. These inclusions provide invaluable insights into the conditions and dynamics of the early Solar System. CAIs must be transported from their formation region near the protosun to the chondrite parent-body accretion region. The nature of their journey could affect how, when, and where the secondary processes recorded in these CAIs occurred [4]. Did these secondary processes occur in the solar nebula or during accretion with the parent body, or both? How were the CAIs affected by varying thermochemical processes? To better answer these questions, we have undertaken an in-depth, textural study of the secondary alteration of select CAI samples.

Methods: We chose three CAIs that experienced a range of post-formation processing to gain better understanding of secondary alteration based on previous preliminary examination [5]. Representative CAIs were chosen from NWA 5508 (CV3), NWA 12772 (CV3), and Coolidge (CL4) carbonaceous chondrites. We used scanning electron microscopy (SEM) and electron backscatter diffraction (EBSD) techniques for detailed chemical, mineralogical, and textural analysis of the CAIs. Backscattered electron (BSE) images and X-ray elemental maps were taken of Coolidge and NWA 5508 using the Lunar and Planetary Institute (LPI) Phenom SEM. The JEOL 7900F SEM at NASA Johnson Space Center (JSC) was used to obtain energy dispersive spectroscopy (EDS) chemical maps of all samples. High resolution EBSD analysis identified the mineral phases and textures, providing key information on their nature. Based on the SEM and EBSD data, minerals of interest were selected for quantitative chemical electron probe micro-analysis (EPMA) using the JEOL JXA-8530F at NASA JSC.

Results and Discussion: The EDS maps show that the NWA 5508 and NWA 12772 CAIs designated "Saguaro" and "Hoopoe" respectively [5] are enriched in calcium while the Coolidge CAI designated "Cottonwood" is aluminum and magnesium rich.

Saguaro. A ~1.5cm diameter igneous Type B CAI with a rounded shape. The dominant phases are melilite, spinel, and Al-Ti pyroxene with minor anorthite. Spinel is subhedral and occurs in clusters. Some of these clusters have a circular geometry which encloses other minerals, known as a palisade structure [6] **(Fig. 1**). Some palisades form near perfect circles while others are more irregular in shape. Melilite in Saguaro ranges in size from coarse (>250μm) to fine-grained (5-7μm) and forms intergrown laths. A third of the melilite grains exhibit simple twinning about their <001> axis.

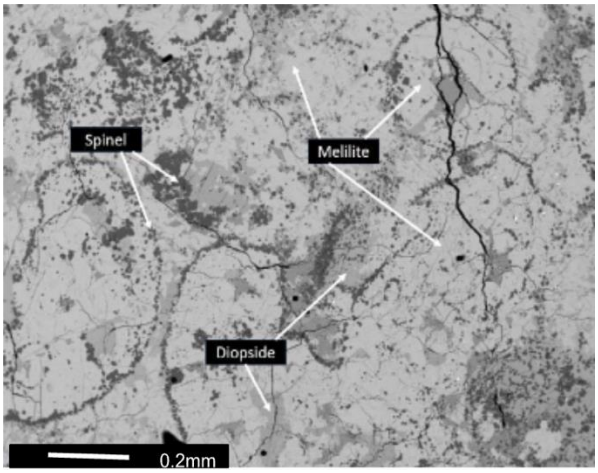

Figure 1: BSE image of spinel palisades in Saguaro

The spinel palisades and twinned melilite in Saguaro suggest an igneous history, and the lack of secondary minerals suggests minimal aqueous alteration. At some point in time after the initial condensation of the minerals and formation of the inclusion, the sample was remelted and quickly solidified. The formation of the palisades is still heavily debated. One hypothesis is that the palisades are the rims of smaller CAIs that accreted early on, essentially acting as xenoliths within the larger CAIs [7]. Another hypothesis suggests an igneous origin for palisade structures [6-8] wherein the melt traps gas bubbles, and the spinel nucleates on the surface of this bubble. Based on the WDS spot analyses of 41 melilite grains using EPMA, the data suggest that the composition inside and outside the palisades is nearly identical. This finding indicates that these palisades are likely not exogenous but rather formed from melt-vapor reactions. Our results are consistent with studies by Simon and Grossman,1997 [6] and Zhang et al. (2019) [8].

Hoopoe. A ~0.5cm compact Type A CAI with an

irregular shape. The dominant mineral phases are melilite, spinel, and hibonite with minor amounts of anorthite, augite, and perovskite. The melilite ranges in size from ~500 to 50μm. The larger melilite grains have simple twinning along the <001> axis like melilite in Saguaro. Melilite in Hoopoe exhibits crystal-plastic strain with misorientation dominantly about the <010> and <110> axes. Spinel shows subhedral to euhedral morphology and appears in clusters. Hibonite grains are similar to spinel in habit and size but show more plastic strain. The two minerals are often found together with one appearing to replace the other. Perovskite appears in fine grained recrystallized regions alongside fine augite and spinel.

The abundant strain and deformation features in the melilite and hibonite suggest that Hoopoe experienced shock. This shock could have occurred in the nebula [9] or from an impact of another body on the parent body asteroid. The appearance of fine-grained (<10μm) areas of augite, perovskite, and spinel in the dominantly coarse-grained inclusion suggest recrystallization, possibly due to the sudden increase in pressure and temperature.

Cottonwood. This ~0.5cm CAI exhibits distinct mineralogy and textures suggesting a high degree of alteration. It is irregular in shape. The dominant mineral phases are spinel and anorthite with minor amounts of augite and rutile. The two main texture types can be seen in **Fig. 2.** The first type consists of coarse euhedral to subhedral spinel and anorthite. The second includes fine grained spinel, anorthite, rutile, and iron sulfides. Within these fine-grained regions, the anorthite grains are clustered into domains exhibiting the same crystallographic orientation. Rutile exclusively occurs with fine anorthite indicating a potential relationship between the two. Cottonwood has a clear and unbroken Wark-Lovering [10] rim (**Fig. 2)** on one side that consists of a sequence of spinel followed by anorthite and an outer layer of augite.

The abundance of the fine-grained regions containing iron oxides and iron sulfides, secondary phases such as rutile, and oriented anorthite grains is evidence for recrystallization associated with a high degree of thermal metamorphism. The EPMA analyses on both coarse- and fine-grained spinel show that the fine spinel grains are more enriched in Cr (1-2 wt. %) than their coarse counterparts (0.1-0.5 wt. %). The data suggest thermal metamorphism drove chemical exchange of the previously refractory inclusion, introducing chromium and iron as well as sulfur, which is moderately volatile.

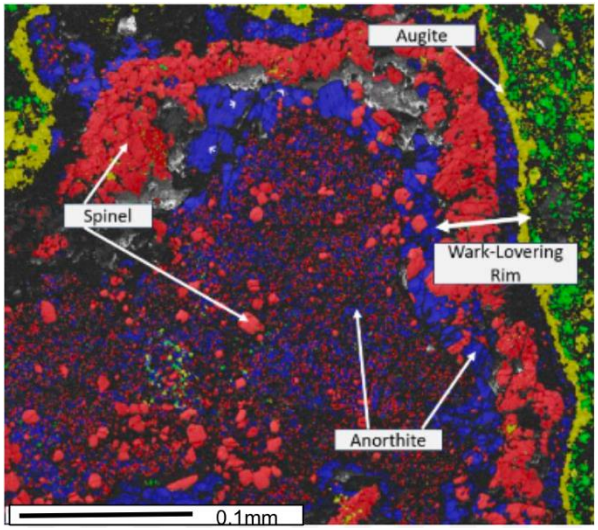

Figure 2: Phase map of minerals found in the rim area of Cottonwood. Both the fine- and coarse-grained spinel (red) and anorthite (blue) domains are visible. Augite (yellow) separates the CAI from the olivine (green) chondrite matrix.

Conclusions: The three CAIs analyzed record distinct secondary nebular and parent body processes. Saguaro melted in the nebula as seen by the twinned melilite and spinel palisades. Hoopoe experienced intense shock which deformed its melilite and recrystallized perovskite, augite, and spinel in fine-grained regions. Cottonwood shows evidence of recrystallization and chemical changes consistent with thermal metamorphism occurring after accretion into the parent-body.

Acknowledgements: We would like to thank Dr. Jen Gorce for her assistance with the analysis and the NFAR through PSEF program for their analytical support. This work was supported by the LPI Summer Intern Program in Planetary Science and the LPI Cooperative Agreement.

References: [1] MacPherson G. J. (2014) *Meteorites and Cosmochemical Processes, Vol. 1 of Treatise on Geochemistry, Elsevier, 2,* 139-179. [2] Grossman L. (1980) *Ann. Rev. Earth Planet. Sci., 8,* 559-608. [3] McSween H. Y. and Huss G. R. (2021) *Cosmochemistry, Cambridge University Press, 2,* 2-4, 110-121, 142-148. [4] MacPherson G. J. et al. (2005) *ASP Conference Series, 341,* 225-250. [5] Mouti Al-Hashimi X. (2023) *LPSC, 54.* [6] Simon S. B. and Grossman L. (1997) *Meteoritics & Planetary Science, 32,* 61-70. [7] Lin Y. and Kimura M. (2000) *Geochimica et Cosmochimica Acta, 64, 23,* 4031-4047. [8] Zhang M. et al. (2019) *Meteoritics & Planetary Science, 54, 5,* 1009-1023. [9] Mane P. et al. (2022) *Geochimica et Cosmochimica Acta, 332,* 369-388. [10] Wark D. A. and Lovering J. F. (1977) *Proc. Lunar Sci. Conf., 8,* 95-112.